



A variational phase field method for curve smoothing

Liyong Zhu^a, Yu Wang^a, Lili Ju^{b,1}, Desheng Wang^{a,*,2}

^a Division of Mathematical Sciences, School of Physical and Mathematical Sciences, Nanyang Technological University, Singapore 637371, Singapore

^b Department of Mathematics, University of South Carolina, Columbia, SC 29208, USA

ARTICLE INFO

Article history:

Received 18 May 2009

Received in revised form 15 October 2009

Accepted 30 November 2009

Available online 11 December 2009

Keywords:

Phase field model

Curve smoothing

Feature preservation

Finite element approximation

Weight function

ABSTRACT

A variational phase field model is proposed for curve smoothing, in which a weight function is associated with the similarity measure term in the model so that important geometric features could be well preserved. Finite element approximation of the proposed model is given for its numerical implementation. Since the model has a linear weak variational form, the discretized system could be solved efficiently by many existing solution techniques. An effective algorithm is also developed, for the purpose of feature preservation, to automatically determine the weight from the given data. Various numerical examples are presented to demonstrate effectiveness and robustness of the proposed method.

© 2009 Elsevier Inc. All rights reserved.

1. Introduction

The problem of *geometry smoothing* or *fairing* such as curve/surface smoothing is of importance in a wide range of fields of science and engineering. For instances, following an image segmentation process, the boundary of the identified object usually has many zigzags and spurious components as shown in Fig. 1; due to sampling errors of physical equipments or some other problems, curves or surfaces extracted from images produced by volumetric MRI or 3D laser scanners inevitably suffer from noises as well [5,13,16]. In order to do further analysis, we often have to smooth out the resulting geometry models. It is indeed these particular applications that motivate the work discussed in this paper.

Partial differential equation (PDE) based methods have gained great attention and success in geometry smoothing. Existing approaches fall into two categories: one is evolution and the other is optimization. The main idea of evolution-based approaches is borrowed from linear heat equations. This technique was originally transplanted into image denoising, called the “P&M diffusion” [15], and in turn extended to geometry smoothing. In [16] Taubin discussed a discretized version of the Laplacian operator on surface meshes. Desbrun et al. [5] used an implicit scheme to obtain a stable diffusion algorithm. Clarenz et al. [4] introduced a process called “anisotropic geometry diffusion” to enhance geometric features of the object while smoothing out noises. Some other evolution-based techniques are discussed in [1,11]. All these methods are carried out on a discretized manifold. In optimization-based approaches, one first constructs an optimization problem that minimizes certain energy functional [12,20], and then the goal of smoothing is attained by solving linear or nonlinear PDEs derived from the corresponding variational formulation. The optimization-based approaches usually have well-founded mathematical foundation which may alleviate the need for developing heuristics, and more important, can be easily incorporated into other re-construction tasks.

* Corresponding author.

E-mail addresses: liyongzhu@hotmail.com (L. Zhu), flimanadam@gmail.com (Y. Wang), ju@math.sc.edu (L. Ju), desheng@ntu.edu.sg (D. Wang).

¹ This author's research is partially supported by the US National Science Foundation under Grant Number DMS-0913491.

² This author's research is partially supported by Singapore MOE ARC 29/07 T207B2202, MOE RG 59/08 M5211092 and NRF 2007IDM-IDM 002-010.

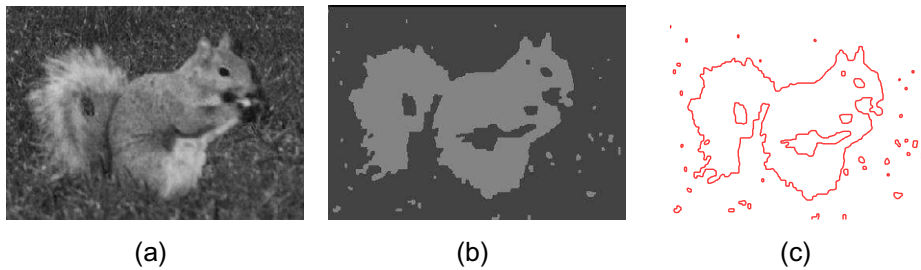


Fig. 1. Segmentation of a squirrel image. (a) The original image; (b) the segmented image; and (c) the noisy object boundary.

Among various optimization-based techniques, the level-set method is widely employed to define the energy functional by expressing some geometry information such as normal, tangent and curvature in term of the distant function [14]. A major advantage of the level-set formulation is its topology-free property, which makes it suitable for processing very complex shapes with topology change. Motivated by the level-set approach, several phase field models [3,6–10,18] were recently developed based on a general energetic variation framework. Similar to the level-set formulation, representing curves implicitly enables the phase field method to easily handle changes of topologies. When the transition width between two phases approaches zero, the phase field model with diffuse-interface gradually becomes identical to a sharp-interface level-set formulation and then it can be reduced properly to a classical sharp-interface model. Since all computations can be performed on a fixed regular mesh, the difficult implementation issues such as re-meshing needed by front tracking type methods can be avoided.

In this paper, a novel phase field model for curve smoothing is proposed, whose energy functional consists of a regularity measure term and a similarity measure term; in particular, the approximated symmetric area difference is used in the similarity measure together with a data-dependent weight function in order to preserve important geometric features such as corners of the curve during the smoothing process. This idea differs from some previous works [4,17,20] in the sense that instead of decreasing the diffusion effect, controlling the effect of the external force is considered. More remarkably, we developed an effective algorithm for determination of the weight, in which the weight is computed automatically from the given noisy curve without any artificial interference. An advantage of the proposed phase field model over the level-set formulation developed in [20] is that the weak variational form derived from the proposed model is linear, which enables us to employ existing simple and efficient numerical solution techniques with solid mathematical foundations. A finite element method is used to discretize and numerically solve the phase field model in this paper. We note that the method developed in the paper also can be extended to surface smoothing without much extra effort.

The rest of this paper is organized as follows. In Section 2, a novel phase field model for curve smoothing is first proposed together with its finite element approximation. Then in Section 3 we develop an effective algorithm for automatical determination of the weight function associated with the similarity measure from the given data so that important geometric features of the original noisy curve can be preserved during the smoothing process. In Section 4 various numerical examples are presented to demonstrate effectiveness and robustness of the proposed method. Finally, concluding remarks are given in Section 5.

2. A phase field model for curve smoothing

In this section, we first recall the abstract model for curve smoothing, and present a variational phase field model with varying weight across the physical domain. The weight function is associated with the similarity measure in the energy functional and its value at each point is usually determined by using information from neighborhood of the point. A finite element method is then employed to discretize the proposed phase field model.

2.1. The phase field model with varying weight

A curve smoothing model is usually formulated as certain functional which can be presented in an abstract manner [20]:

$$\Gamma = \operatorname{argmin}(\operatorname{regularity}(\Gamma) + \operatorname{similarity}(\Gamma, \Gamma_0)), \quad (1)$$

where Γ_0 and Γ denote the initial noisy curve and the final smoothed one, respectively. The first term is a regularity measure of Γ while the second one is a similarity measure between Γ and Γ_0 . The similarity term plays a role as an external force controlling the *distance* or *difference* between the noisy and smoothed curves. The solution (smoothed) curve Γ must be the minimizer of the above functional (1).

As in [18], we use a phase function ϕ defined on the physical domain Ω containing the curve Γ to implicitly represent the curve Γ . The phase function ϕ has various phases across the domain Ω – it basically takes positive value inside Γ and negative value outside. Between these two phases there is a transition layer. Thus, the phase function can be naturally employed to label the inside or outside of the curve Γ . The level-set $\{x|\phi(x) = 0\}$ gives the curve, while $\{x|\phi(x) > 0\}$ represents the inside of the curve Γ and $\{x|\phi(x) < 0\}$ the outside.

With such a phase function ϕ , we may define the regularity term as in [20] by the following formulation:

$$\text{regularity}(\Gamma) = \frac{\epsilon}{2} \int_{\Omega} |\nabla \phi(x)|^2 dx. \quad (2)$$

It is shown in [18] that the formulation (2) is approximately proportional to the *length of the curve*, $|\Gamma|$, when the phase function $\phi(x)$ has the form $\phi(x) = \tanh(d(x, \Gamma)/\sqrt{2}\epsilon)$. Here $d(x, \Gamma)$ is the signed distance of x to the curve Γ and ϵ the width of transition layer.

For the similarity term, the *symmetric area difference* of regions surrounded by the initial curve Γ_0 and the smooth one Γ , respectively, is a natural choice as suggested in [20]. Assume that ϕ_0 is a phase function representing the initial noisy curve. Then the following formulation may be employed as the similarity term

$$\text{similarity}(\Gamma, \Gamma_0) = \frac{1}{2} \int_{\Omega} (\phi(x) - \phi_0(x))^2 dx, \quad (3)$$

which is a good approximation to the symmetric difference of areas surrounded by Γ and Γ_0 . Using (2) and (3), we then can define a *basic phase field model* for curve smoothing as follows:

$$\min_{\phi} \mathcal{E}_0(\phi) = \frac{\epsilon}{2} \int_{\Omega} |\nabla \phi(x)|^2 dx + \frac{\lambda}{2} \int_{\Omega} (\phi(x) - \phi_0(x))^2 dx, \quad (4)$$

where $\lambda > 0$ is a constant weighting parameter and added to control the closeness of the resulting curve to the noisy curve.

In many applications, feature preservation when fairing curves or surfaces is often very important. As shown by many examples in [20], a major disadvantage of the above basic curve smoothing model (4) is that important geometric features such as corners of the curve are often eliminated along with noises during the smoothing process when a constant weighting parameter λ over the whole physical domain is used. Several anisotropic diffusion models were recently proposed for avoiding this problem. Basically all existing anisotropic diffusion approaches are based on the simple principle that the diffusion effect should be small in the feature regions. In [4,17] the authors tried to achieve this goal by a properly designed diffusion function which changes the diffusion coefficient across different regions. On the other hand, it is worth noting [20] that changing the diffusion effect is almost equivalent to changing the weighting parameter λ associated with the similarity measure in (4).

Inspired by the above work, we propose the following modified model of (4), called a *phase field model with varying weight* as follows:

$$\min_{\phi} \mathcal{E}(\phi) = \frac{\epsilon}{2} \int_{\Omega} |\nabla \phi(x)|^2 dx + \frac{1}{2} \int_{\Omega} \lambda(x) (\phi(x) - \phi_0(x))^2 dx, \quad (5)$$

where a weight function $\lambda(x) > 0$ is used instead of a constant parameter. The question about how to appropriately determine $\lambda(x)$ for a given noisy curve so that corner information could be well preserved will be addressed in the next section. Thus, the original problem of curve smoothing can be formulated as finding the function $\phi = \phi(x)$ defined on the domain Ω that minimizes the functional $\mathcal{E}(\phi)$. It is easy to see that the functional $\mathcal{E}(\phi)$ is strictly convex, and we have the following theorem on the existence of the minimizer of $\mathcal{E}(\phi)$.

Theorem 2.1. *The minimization problem defined by (5) has a unique minimizer.*

2.2. Finite element approximation of the phase field model

Assume that the minimization problem (5) has a minimizer $\phi \in H_0^1(\Omega)$, then ϕ can be characterized by the following weak variational formulation:

$$a(\phi, \psi) = \int_{\Omega} \lambda(x) \phi_0(x) \psi(x) dx, \quad \forall \psi \in H_0^1(\Omega), \quad (6)$$

where

$$a(\phi, \psi) = \epsilon \int_{\Omega} \nabla \phi(x) \cdot \nabla \psi(x) dx + \int_{\Omega} \lambda(x) \phi(x) \psi(x) dx.$$

According to the standard Lax–Milgram theory [2], we have the following theorem on well-posedness of the above weak variational formulation:

Theorem 2.2. If $\phi_0 \in L^2(\Omega)$, then the weak variational formulation defined by (6) has a unique solution ϕ in $H_0^1(\Omega)$.

To construct a finite element approximation of the weak variational formulation (6), we take a discrete function space

$$V_h = \{v_h \in C^0(\Omega) \cap H_0^1(\Omega) | v_{h|_K} \in P_k(K), \forall K \in J_h\}, \tag{7}$$

where J_h is a uniformly regular triangulations of $\bar{\Omega}$ consisting of triangles K whose diameters are bounded above by the mesh size parameter h , and P_k denotes the space of all polynomials of degree not larger than k . Then the finite element approximation of (6) is to find $\phi_h \in V_h$ such that

$$\epsilon \int_{\Omega} \nabla \phi_h(x) \cdot \nabla \psi_h(x) dx + \int_{\Omega} \lambda(x) \phi_h(x) \psi_h(x) dx = \int_{\Omega} \lambda \phi_0(x) \psi_h(x) dx, \tag{8}$$

for any $\psi_h \in V_h$. The resulting linear system is symmetric positive definite and can be efficiently solved by the preconditioned conjugate gradient or algebraic multi-grid method.

For easy reference, we name the above algorithm the *phase field method for curve smoothing* (PFMCS). According to the finite element theory, convergence of the solution of (8) can be proved by standard arguments (see [2]):

Theorem 2.3. The finite element approximation (8) of the weak variational formulation (6) has a unique solution $\phi_h \in V_h$ and ϕ_h satisfies the following error estimates:

$$\|\phi - \phi_h\|_{s,\Omega} \leq Ch^{k+1-s} \|\phi\|_{k+1,\Omega}, \quad 0 \leq s \leq k, \tag{9}$$

where $\|\cdot\|_{s,\Omega}$ denotes the standard Sobolev space norm.

We also note that the strong form of the Euler–Lagrange equation for the minimization problem (5) is given by

$$-\epsilon \Delta \phi(x) + \lambda(x)(\phi(x) - \phi_0(x)) = 0 \tag{10}$$

with certain Dirichlet boundary conditions. Thus, the system (6) may also be viewed as a weak variational formulation of (10).

3. Determination of the weight $\lambda(x)$

The remaining important question is how to appropriately choose the weight function $\lambda(x)$ for a given data (a noisy curve) so that geometric features of the curve such as corners can be well preserved during the smoothing process. Provided that a proper corner detector is available, this can be achieved by specifying a non-homogeneous “attraction potential” which makes corner more attractive – setting the weight $\lambda(x)$ large in regions near corners and small in flat regions. Discrete curvature could be one of good corner detectors in many applications, but since the raw datum are usually eroded by noises in geometry smoothing cases, point-wise evaluation or approximation of the curvature is not reliable at all. Inspired by the neighborhood idea proposed in [19], a similar *averaging technique* is utilized in this paper to overcome this hurdle in designing the corner detector.

We first describe the main idea behind our approach. Let $x \in \Omega$ be a concerning point. A reference circle $S(x)$ centered at the point x is introduced for the “averaging” purpose – for removing effects caused by noises and detecting corners. If the boundary (smooth) curve Γ does not pass through $S(x)$, then clearly x is not close to the boundary Γ and therefore $\lambda(x)$ should be small. Now, let us concentrate on the situation of the reference circle $S(x)$ being divided into two parts A and B by Γ . First we suppose that the part of Γ intersecting $S(x)$ is quite straight (i.e. curvature is small); There are totally three cases, see Fig. 2 for an illustration. In these cases $\lambda(x)$ should be small without a doubt. If a corner of Γ is contained inside of $S(x)$, then we must be much more careful; see Fig. 3 where four such cases are presented. We think $\lambda(x)$ should be small for the second and fourth cases since x is not very close to the corner, but $\lambda(x)$ should be large for the first and third cases. The above observations also basically hold for the case of a noisy curve if the radius of the circle is large enough to cover the amplitude of noises.

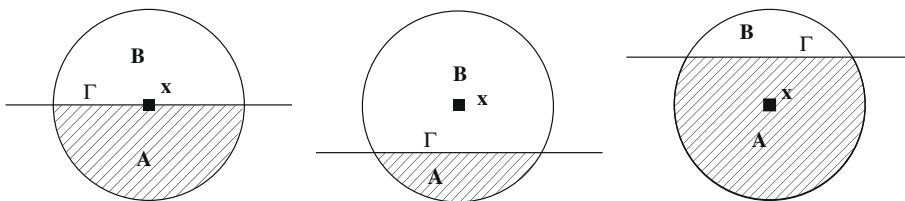


Fig. 2. A quite straight part of Γ passes through $S(x)$ (i.e. no corner is present). Left: $Area(A) - Area(B) \approx 0$; middle: $Area(B) - Area(A) > 0$ and $\phi(x) = \phi(B)$; right: $Area(A) - Area(B) > 0$ and $\phi(x) = \phi(A)$.

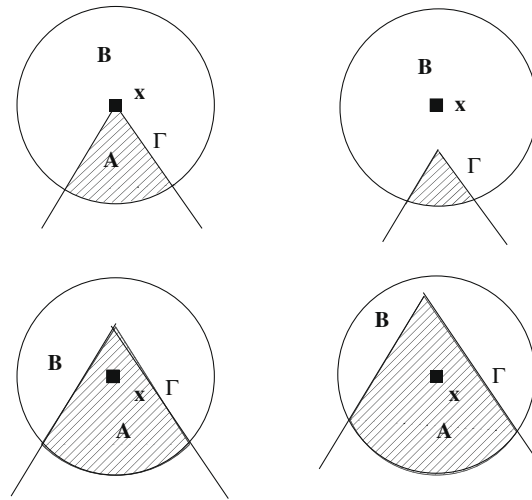


Fig. 3. A highly curved part of Γ passes through $S(x)$ (i.e. a corner is present). Top-left: $|Area(A) - Area(B)| \approx (1 - \alpha/\pi)Area(S(x))$ where α denotes the angle of the corner; top-right: $Area(B) - Area(A) > 0$ and $\phi(x) = \phi(B)$; bottom-left: $Area(A) - Area(B) \approx 0$; bottom-right: $Area(A) - Area(B) > 0$ and $\phi(x) = \phi(A)$.

In the following, we present an algorithm for determination of the weight $\lambda(x)$ using local information around x . Denote J_h as a triangulation of the computational domain Ω with nodes $\{v_i\}$.

Algorithm 1. (Determination of $\lambda(x)$):

1. For every node $v_i \in J_h$ in the computational domain Ω :
 - (a) choose a reference circle $S(v_i, r)$ centered at v_i with a radius r ;
 - (b) count the number of nodes, $N = N^+ + N^-$, contained inside the reference circle $S(v_i, r)$ where N^+ denotes the number of nodes with a positive phase value ($\phi_0 > 0$) in $S(v_i, r)$ and N^- that with a negative phase value ($\phi_0 < 0$). Set $N_{\min} = \min\{N^+, N^-\}$;
 - (c) if $N_{\min} = N^+$ and $\phi_0(v_i) > 0$ or $N_{\min} = N^-$ and $\phi_0(v_i) < 0$, then set $s(v_i) = N_{\min}/N$, otherwise, $s(v_i) = 1/2$;
 - (d) set

$$\lambda(v_i) = f(s(v_i)), \tag{11}$$

where $f(s)$ is a continuous positive function defined on $[0, 1]$.

2. Interpolate $\lambda(v_i)$ based on the triangulation J_h to get a piecewise linear function $\lambda(x)$ which will be used in the finite element approximation (8).

In practical implement of Algorithm 1, two things need to be carefully considered. The first one is the choice of the function $f(s)$. It is expected that $f(s(x))$ is small when the curve is relatively straight which means that $f(s(x))$ should attain its minimum at $s = 1/2$. Meanwhile, it is also expected that $f(s(x))$ changes dramatically with respect to $s(x)$ so as to produce big difference between corner points and the other points. In our experiments, $f(s)$ is chosen to be

$$f(s) = \lambda_0 e^{w(1-2s)^2}, \tag{12}$$

where λ_0 and w are some given positive constants. The function (12) gives $f(s) = \lambda_0$ when $s = 1/2$, and changes rapidly when s goes away from $1/2$. Another possible candidate is

$$f(s) = \lambda_0(1 + w(1 - 2s)). \tag{13}$$

The other issue is the choice of the radius r of the reference circle $S(v_i, r)$. To characterize corners of the curve, the reference circle should be large enough so as to suppress the influence of noises. On the other hand, too large r may lead to a lot of unnecessary computation cost and give inaccurate results especially when $S(v_i, r)$ contains more than one corner. Usually, one may start from a small circle, and gradually increases the radius until a satisfactory result is achieved. In practice, when x is not close enough to a corner of the boundary curve Γ , $s(x)$ calculated by the proposed algorithm is often quite small. In order to make the sharp corners more distinguishable, a threshold can be set such that $s(x)$ is assigned to be zero when $s(x)$ falls below that threshold.

The proposed Algorithm 1 works well except for outliers which might be wrongly recognized as corners by the algorithm. To eliminate such an undesirable effect, the following extra process for detecting outliers can be added into Algorithm 1:

Algorithm 2. (Detection of outliers):

For every node $v_i \in J_h$ in the computational domain:

- (a) choose the reference circle $S(v_i, r_1)$ and count the number of nodes, $N_1 = N_1^+ + N_1^-$, contained inside $S_1(v_i, r_1)$;
- (b) increase the radius of the circle to r_2 , and count the number of nodes, $N_2 = N_2^+ + N_2^-$, contained inside $S(v_i, r_2)$;
- (c) if $N_1^+ \approx N_2^+$ or $N_1^- \approx N_2^-$, then v_i is regarded as a outlier and set $s(v_i) = 1/2$; otherwise, $s(v_i)$ is remained unchanged (evaluated by Algorithm 1).

We set $r_2 = 2r_1$ in our numerical experiments. For curves with outliers, Algorithm 1 is applied and followed by Algorithm 2 so that the weight $\lambda(x)$ of normal points and outliers can be correctly computed. In the following section, various examples will be applied to test and evaluate our PFMCS method.

4. Numerical experiments

The proposed phase field method for curve smoothing with the linear finite element approximation is implemented using C Language. We note that the resulting linear system is solved by a AMG solver from AFEPack (<http://www.acm.caltech.edu/~rli/AFEPack/>). The computational domain is $\Omega = [0, 1] \times [0, 1]$. We set the transition parameter $\epsilon = 0.01$ and use a uniform structured triangular mesh of Ω with 400×400 nodes so that the mesh is fine enough to resolve the transition layers very well. High-order Gaussian quadrature points are used in our experiments to evaluate numerical integrations of the phase function and basis functions.

In the following, the PFMCS method is investigated by experiments in which corners of the given curves are desired to be preserved during the smoothing process; in particular, the PFMCS method with varying weight will be compared with that with constant weight to demonstrate its big advantage over the latter one. We will always take the form of (12) for $f(s)$ in Algorithm 1 for computing the weight function $\lambda(x)$ when needed.

4.1. Two basic examples

The curve shown in Fig. 4(b) is a noisy H-shape curve. It is obtained by randomly perturbing a clear H-shape curve (see Fig. 4(a)). We note there is no noise around the twelve corners of the curve, which make it convenient to test whether the PFMCS method with varying weight can preserve these corners. The weight function $\lambda(x)$ is determined by Algorithm 1 with $\lambda_0 = 12$, $r = 0.075$ and $w = 25$; see Fig. 4(c) and (d) for visualization of $\lambda(x)$. It is clear that $\lambda(x)$ has larger values around the corners. The smoothed H-shape curve obtained by the PFMCS method with such weight is given in Fig. 5(a) and it shows that

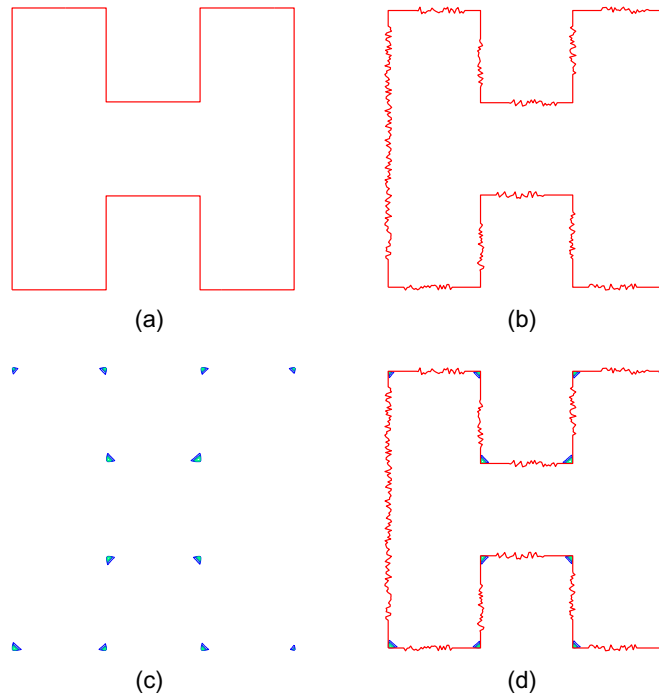


Fig. 4. A noisy H-shape curve and the corresponding weight $\lambda(x)$ calculated using Algorithm 1. (a) The original clear curve; (b) the initial noisy curve; (c) contour of the corresponding weight; and (d) mixture of the noisy curve and the weight contour.

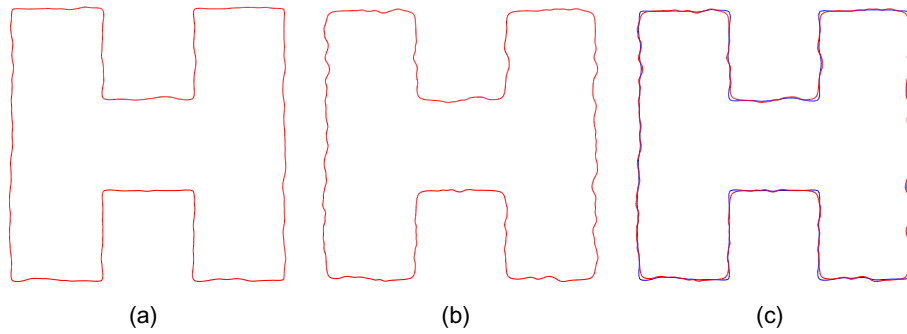


Fig. 5. Smoothing of a noisy H-shape curve by the PFMCs method. (a) The smoothed curve using varying weight; (b) the smoothed curve using constant weight; (c) comparison of the two smoothed curves (the curve using varying weight is colored with blue). (For interpretation of the references to colour in this figure legend, the reader is referred to the web version of this article.)

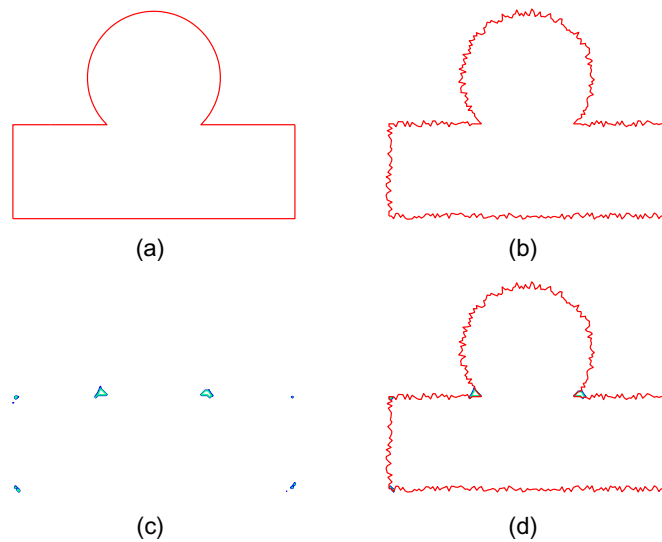


Fig. 6. A noisy “Circ-Rect” curve and the corresponding weight $\lambda(x)$ calculated using Algorithm 1. (a) The original clear curve; (b) the initial noisy curve; (c) contour of the corresponding weight; and (d) mixture of the noisy curve and the weight contour.

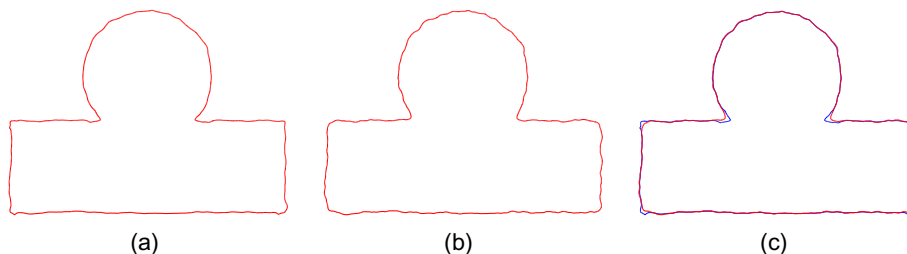


Fig. 7. Smoothing of a noisy “Circ-Rect” curve by the PFMCs method. (a) The smoothed curve using varying weight; (b) the smoothed curve using constant weight; (c) comparison of the two smoothed curves (the curve using varying weight is colored with blue). (For interpretation of the references to colour in this figure legend, the reader is referred to the web version of this article.)

the noises are removed effectively as well as all its twelve corners being well preserved. It is easy to see that the smoothed curve is an excellent approximation to the original clear one. In addition, the smoothed curve by the PFMCs method with constant weight $\lambda(x) \equiv 75$ is also presented in Fig. 5(b), which shows that corners of the rectangle are smeared out. For the purpose of comparison, the above two smoothed curves are put together in Fig. 5(c), which demonstrates that the PFMCs method with varying weight easily outperforms that with constant weight. It is variation of the weight function $\lambda(x)$ that makes such a big difference in smoothing results.

In Figs. 6 and 7, a noisy curve (denoted by “Circ-Rect”) formed by gluing parts of a circle and a rectangle is smoothed by the PFMCS method. The noisy curve presented in Fig. 6(b) is again produced by randomly perturbing a clear version of the corresponding “Circ-Rect” curve (see Fig. 6(a)), and we specially note that the noise is present on the whole curve in this example. The PFMCS method with varying weight is first tested. We set $\lambda_0 = 40, r = 0.0375$ and $w = 40$ in the function (12) and the weight function $\lambda(x)$ obviously has larger values in regions close to the corners as seen in Fig. 6(c) and (d). From the resulting smoothed curve presented in Fig. 7(a), we easily observe that the proposed method preserves all corners effectively during the smoothing process and produces a good approximation to the original clear curve at the same time. Compared with the resulting curve by the PFMCS method with constant weight $\lambda(x) \equiv 150$ (see Fig. 7(b) and (c)), the former approach clearly does better in preserving the sharp corners.

In the following, we will quantitatively justify our observations in the above two examples. Denote by C_{clear} the original clear curve (without any noise) and by C_{smooth} the smoothed version of the initial noisy curve by using the PFMCS method. A distance between C_{clear} and C_{smooth} can be defined quantitatively by

$$Dist(C_{clear}, C_{smooth}) = \frac{A_{diff}}{A_{clear}},$$

where A_{diff} is the symmetric area difference of the regions enclosed by the curves C_{clear} and C_{smooth} , and A_{clear} is the area of the region surrounded by C_{clear} . The quantity $Dist(C_{clear}, C_{smooth})$ is in fact the normalized symmetric area difference. Denote by N_{diff} the number of mesh points on which the phase functions representing the curves C_{clear} and C_{smooth} respectively have different signs, and by N_{clear} the number of mesh points on which the phase function representing C_{clear} has a positive sign. When the (uniform) mesh is fine enough, we have

$$Dist(C_{clear}, C_{smooth}) \approx \frac{N_{diff}}{N_{clear}}. \tag{14}$$

It is clear that the smaller $Dist(C_{clear}, C_{smooth})$ is, the closer two curves are (i.e. the magnitude of $Dist$ shows how good a denoising result is).

Table 1 contains the statistics of the normalized symmetric area difference $Dist(C_{clear}, C_{smooth})$ computed for the H-shape and “Circ-Rect” curve examples. For the H-shape curve example, we listed results by the PFMCS method with constant weights $\lambda(x) \equiv 25, 50, 75, 150, 200$, respectively, and the varying weight used above, $\lambda(x) = 12e^{25(1-2s(x))^2}$; for the “Circ-Rect” curve example, we reports results by the PFMCS method with constant weights $\lambda(x) \equiv 50, 100, 150, 200, 250$, respectively, and the varying weight $\lambda(x) = 40e^{40(1-2s(x))^2}$. It is clear in both examples that the smoothed curve obtained by the PFMCS method with varying weight gives the minimum $Dist(C_{clear}, C_{smooth})$.

4.2. More complicated examples

In the following we will investigate performance of the PFMCS method for more complicated examples. Fig. 8(a) shows a noisy polygonal curve and Fig. 8(b) and (c) presents the corresponding weight $\lambda(x)$ with $\lambda_0 = 40, r = 0.1$, and $w = 20$. It can be observed that due to the influence of noises the contour of $\lambda(x)$ has very large effecting area around some sharp corners, and for some natty corners it even shrinks to a point. This is partly because the noises around the sharp corners have almost the same amplitude as the corners so that the proposed algorithm hardly differentiates corners from noises. The smoothed curve by the PFMCS method with varying weight is given in Fig. 9(a). We also compare it with the result by the PFMCS method with constant weight $\lambda(x) \equiv 40$ in Fig. 9(b) and (c). The resulting curve does preserve all corners well, but some noises are also kept after smoothing in regions close to the corners, especially the sharp corners. A obvious compromise is to decrease the parameters λ_0 in (12) in order to get smoother results.

The next example is a noisy eight-sided star, as shown in Fig. 10(a), with many outliers. If only Algorithm 1 is applied, the outliers will be wrongly recognized as corners. For instance, in Fig. 10(b) the outliers are kept as well as corners. In this case, Algorithm 2 has to be applied to further detect outliers and modify the corresponding weights. Fig. 10(c) shows the result

Table 1
The normalized symmetric area difference $Dist(C_{clear}, C_{smooth})$.

<i>H-shape curve</i>					
Constant weight	$\lambda = 25$	$\lambda = 50$	$\lambda = 75$	$\lambda = 150$	$\lambda = 200$
$Dist(C_{clear}, C_{smooth})$	0.0230	0.0173	0.0165	0.0168	0.0176
Varying weight	$\lambda(x) = 12e^{25(1-2s(x))^2}$				
$Dist(C_{clear}, C_{smooth})$	0.0059				
<i>“Circ-Rect” Curve</i>					
Constant weight	$\lambda = 50$	$\lambda = 100$	$\lambda = 150$	$\lambda = 200$	$\lambda = 250$
$Dist(C_{clear}, C_{smooth})$	0.0172	0.0130	0.0121	0.0122	0.0125
Varying weight	$\lambda(x) = 40e^{40(1-2s(x))^2}$				
$Dist(C_{clear}, C_{smooth})$	0.0080				

...since they are elongated and keep them during the process. However, by using the characters of "N" and "..." identified as important features and therefore preserved as shown in the figure.

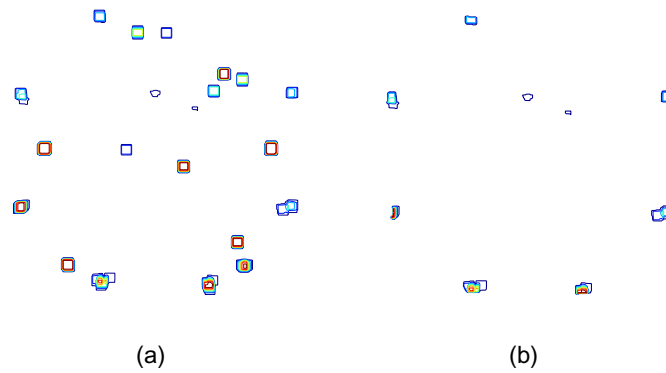


Fig. 11. Comparison of the weight functions. (a) Contour of the weight used in Fig. 10(b); and (b) contour of the weight used in Fig. 10(c).

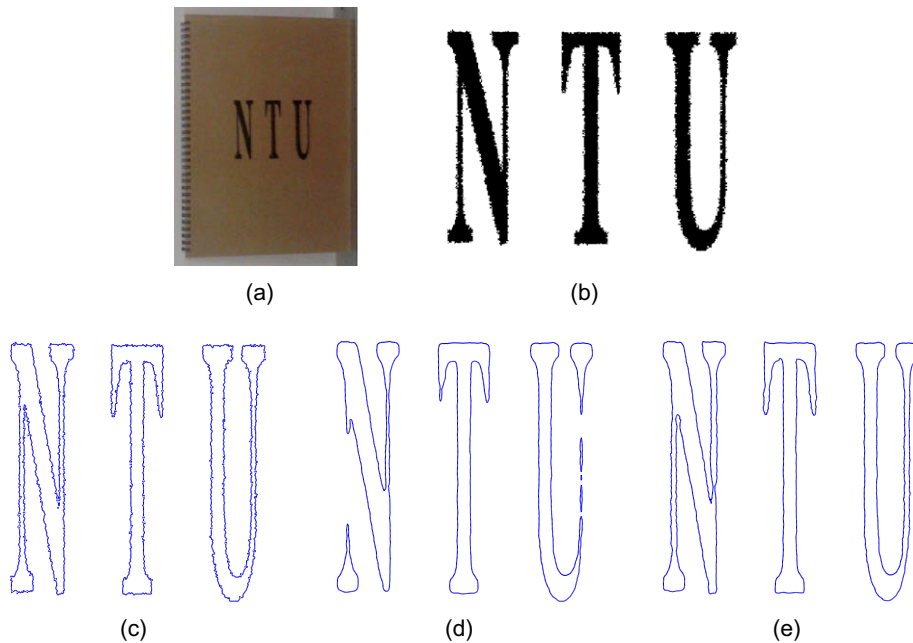


Fig. 12. Segmentation result of an image containing words “NTU” and its smoothed boundary curves by the PFMCs method. (a) The original picture; (b) the segmentation result; (c) boundaries of the object; (d) the smooth curve with constant weight; and (e) the smoothed curve with varying weight.

5. Conclusions and future work

In this paper a novel phase field model and its finite element approximation are proposed for curve smoothing; in particular, the weighting parameter associated with the similarity measure in the energy functional may vary across the whole physical domain such that important geometric features such as corners may be well preserved during the smoothing process. We also develop an algorithm for determination of the weight from the given noisy curve without any artificial interference. These techniques are easy-to-implement and yet very effective. Various numerical examples are presented to demonstrate effectiveness and robustness of the proposed method. It is quite straightforward to extend the method to interesting surface/manifold smoothing in the three-dimensional space, which is still under our investigation. In order to overcome limitation of the mesh resulting from the small transition layer in the phase field model and improve efficiency of the method, adaptive finite element solutions of the proposed model based on a posteriori error estimates will be one of our future research directions as well. Finally, a thorough study of the possible links between TV-regularization [14] and the corner detector proposed in this work is also of great interest.

References

- [1] M. Alexa, Wiener filtering of meshes, in: Proceedings of the Shape Modeling International, 2002, pp. 51–57.
- [2] S. Brenner, L. Scott, The Mathematical Theory of Finite Element Methods, Springer-Verlag, 1996.

- [3] L. Chen, Phase-field models for microstructure evolution, *Ann. Rev. Mater. Res.* 32 (2002) 113–140.
- [4] U. Clarenz, U. Diewald, M. Rumpf, Anisotropic geometric diffusion in surface processing, in: *Proceedings of IEEE Visualization*, 2000, pp. 397–405.
- [5] M. Desbrun, M. Meyer, P. Schröder, A.H. Barra, Implicit fairing of irregular meshes using diffusion and curvature flow, in: *Proceedings of SIGGRAPH*, 1999, pp. 317–324.
- [6] Q. Du, C. Liu, R. Ryham, X. Wang, Phase field modeling of the spontaneous curvature effect in cell membranes, *Commun. Pure Appl. Anal.* 4 (2005) 537–548.
- [7] Q. Du, C. Liu, X. Wang, A phase field approach in the numerical study of the elastic bending energy for vesicle membranes, *J. Comput. Phys.* 198 (2004) 450–468.
- [8] Q. Du, C. Liu, X. Wang, Retrieving topological information for phase field models, *SIAM J. Appl. Math.* 65 (2005) 1913–1932.
- [9] Q. Du, C. Liu, X. Wang, Simulating the deformation of vesicle membranes under elastic bending energy in three dimensions, *J. Comput. Phys.* 212 (2005) 757–777.
- [10] Q. Du, L. Zhu, Analysis of a mixed finite element method for phase field elastic bending energy of vesicle membrane deformation, *J. Comput. Math* 24 (2006) 265–280.
- [11] S. Fleishman, I. Drori, D. Cohen-Or, Bilateral mesh denoising, *ACM Trans. Graphics* 22 (2003) 950–953.
- [12] L. Kobbelt, T. Hesse, H. Prautzsch, K. Schweizerhof, Iterative mesh generation for fe-computations on free form surfaces, *Eng. Comput.* 14 (1997) 806–820.
- [13] S. Rusinkiewicz, O. Hall-Holt, M. Levoy, Real-time 3D model acquisition, *ACM Trans. Graphics* 21 (2002) 438–446.
- [14] S. Osher, R. Fedkiw, *The Level Set Method and Dynamic Implicit Surfaces*, Springer, Berlin, 2002.
- [15] P. Perona, J. Malik, Scale space and edge detection using anisotropic diffusion, *IEEE Trans. Patt. Anal. Mach. Intell.* 12 (1990) 629–639.
- [16] G. Taubin, A signal processing approach to fair surface design, in: *Proceedings of SIGGRAPH*, 1995, pp. 351–358.
- [17] T. Tasdizen, R. Whitaker, P. Burchard, S. Osher, Geometric surface smoothing via anisotropic diffusion of normals, in: *Proceedings of the Conference on Visualization*, 2002, pp. 125–132.
- [18] X. Wang, Phase field models and simulations of vesicle bio-membranes, Ph.D. Thesis, Department of Mathematics, Penn State University, 2005.
- [19] J. Wang, L. Ju, X. Wang, An edge-weighted centroidal voronoi tessellation model for image segmentation, *IEEE Trans. Image Process.* 18 (2009) 1844–1858.
- [20] Y. Wang, S. Song, Z. Tan, D. Wang, Adaptive variational curve smoothing based on level set method, *J. Comput. Phys.* 228 (2009) 6333–6348.